ORIGINAL RESEARCH (AR) DOI: 10.4274/jems.2024.79836

Journal of ETA Maritime Science 2024;12(3):238-252

Quasi-2DH Modeling of the Shoreline Evolution Around an Offshore Breakwater

Cüneyt Baykal, Can Özsoy

Middle East Technical University Faculty of Engineering, Department of Civil Engineering, Ankara, Türkiye

Abstract

In the present study, a quasi-two-dimensional (2D) numerical model developed to model shoreline evolution under wave action near various coastal defense implementations is applied to laboratory experiments on shoreline evolution around an offshore breakwater. The model uses a spectral wave model based on the energy balance equation with wave breaking and diffraction terms. A method is proposed to distribute bulk longshore sediment transport rates over the surf zone for 2D applications. The proposed method agrees with the one-dimensional methods and 2D laboratory measurements. The model also comprises cross-shore and swash zone transport modules for maintaining the equilibrium profile, which is tested using a theoretical case governed solely by cross-shore transport. The test shows that the cross-shore transport module can restore any user-defined equilibrium beach profile. For the laboratory experiments, the model results for the nearshore wave heights and bottom contours agree well with the experimental results, especially for the initial cases of laboratory experiments. As the salient progresses through the offshore breakwater and a tombolo forms, the wave approach and local orientation angles increase, and the computed bottom contours begin to differ from the measured contours.

Keywords: Sediment transport, Shoreline change model, Quasi-2DH, Offshore breakwater

1. Introduction

The ever-increasing development and human interventions in coastal areas have led to significant shoreline changes. Hence, it is imperative to determine shoreline evolution in a specific condition or state to comprehend the associated processes and address them effectively. With recent advancements in computing technology, numerical modeling has become more convenient than ever before. Numerical modeling of shoreline evolution began with the pioneering work of Pelnard-Considere [1]. He defined a mathematical model for predicting the shoreline's position near a groin. This model assumes that nearshore seasonal variations, such as bar formation and storm-induced accretion/erosion, are negligible in the long-term (yearly, decadal) progress of the shoreline. Additionally, equilibrium beach profile represents the entire shoreline, and longshore sediment transport (LST) is the governing process. Price et al. [2] first numerically implemented the one-line theory, followed by many others [3-10].

Wave transformation computations mainly depend on parametric and geometrical relationships in one-line models. Thus, when coastal structures with complicated geometries and conditions are present in the nearshore region, such wave transformation computations become excessively convoluted in one-line models. Nonetheless, two- and three-dimensional numerical models can solve many equations with numerous input parameters, but they suffer from a significant increase in computational complexity. These models may not provide quick/interim solutions for designing and testing the effectiveness of coastal defense measures in time-sensitive studies such as coast restoration projects. However, one-line models may also not be sufficient for modeling highly complex coastal structures, sediment transport in curved shorelines, the effect of topographical conditions, and cross-shore transport, and for predicting tombolo formation, accretion, and erosion around structures such as Y-heads, T-head groins, or combinations of structures. Researchers have applied several methods and models to improve the

Address for Correspondence: Cüneyt Baykal, Middle East Technical University Faculty of Engineering, Department of Civil Engineering, Ankara, Türkiye
E-mail: cbaykal@metu.edu.tr
ORCID iD: orcid.org/0000-0002-8514-2758

Received: 25.12.2023
Last Revision Received: 20.03.2024
Accepted: 12.05.2024

To cite this article: C. Baykal, and C. Özsoy. "Quasi-2DH Modeling of the Shoreline Evolution Around an Offshore Breakwater." *Journal of ETA Maritime Science*, vol. 12(3), pp. 238-252, 2024.

computation of wave transformation around complex structures and bathymetry in one-line models. Hoan [11] coupled the EBED [12] wave model, solving the energy balance equation, with a one-line model to compute wave transformation in the nearshore. Smith [13] used an N-LINE model, in which the model is coupled with the SWAN wave model [14]. Similarly, Kristensen et al. [15] computed the sediment transport fluxes with MIKE21 [16] and integrated those fluxes over the surf zone to compute the sediment transport in the one-line model. Dang [17] incorporated an N-LINE model with RCPWAVE [18], a simple linear wave model, to compute wave characteristics in a large domain. To include the cross-shore transport effects, Hanson et al. [19] and Hanson and Larson [20] added cross-shore modules to one-line models, Larson et al. [21] coupled a beach profile model with a one-line model, Hanson and Larson [22], Dabees and Kamphuis [23], and Dang [17] developed multiple-line models, and Shimizu et al. [24] and van den Berg et al. [25]. Robinet et al. [10,26] developed a grid-based one-line approach using a 2D wave refraction model and a cross-shore transport module. The researchers also studied one major drawback of the one-line models: the shoreline's irregularities tend to smooth out, and curved shorelines become straight. Hanson et al. [27] surpassed this by introducing a stable representative coastline. Larson et al. [28,29] defined a regional shoreline to make the local shoreline progress in alignment with the regional shoreline. They also included a geometric wave transformation tool that transforms the waves into a representative contour. Kaergaard and Fredsoe [30] introduced a vector-based approach to model the evolution of shorelines with significant curvature. They performed detailed computations on sediment transport rates using spectral wave, hydrodynamic, and sand transport models. Several other researchers have also developed more detailed 2D depth-averaged horizontal (2DH) models to resolve the nearshore currents and associated transport rates [31-35]. However, these models required significantly higher computation times than the simple one-line models [36].

The present study investigates a shoreline evolution modeling approach with a more precise computed nearshore wave field around complex coastal structures compared with one-line models while demanding a smaller number of input parameters and less computational source compared with complex 2DH and 3D models, eliminating intense nearshore circulation and advection-diffusion computations. For this purpose, a depth-averaged quasi-2-dimensional shoreline evolution numerical model (Q-2DH hereafter) is constructed on the basis of the 2DH Beach Evolution Model [35] and following the simplified approach of van den Berg et al. [25] to compute nearshore sediment transport. The model is then applied to the laboratory experiments of Gravens and Wang [37] on the shoreline evolution around a detached breakwater, and the computed nearshore wave fields and post-test bathymetries are quantitatively compared with the measurements. This study is compiled from the thesis of the second author.

The paper is organized as follows. Section 2 describes the theoretical background of the Q-2DH model, its structure, and its main assumptions. Section 3 describes the model setup and the simulations conducted. Here, the model is applied to a cross-shore transport-related theoretical benchmark case and to Gravens and Wang's [37] laboratory experiments to investigate morphological changes around a detached breakwater. Finally, in section 5, the results are discussed, and the study conclusions are drawn.

2. Materials and Methods

In this chapter, the theoretical background of the Q-2DH model is described in detail.

2.1. Model Structure

The Q-2DH model is comprised of three main modules: a nearshore spectral wave (NSW) model [38], a sediment transport module (STD), and a morphology evolution module (MEV). MATLAB® is employed to develop the model, which operates on a rectangular grid and utilizes finite difference schematization to solve the governing equations. The Q-2DH model considers several input parameters, such as bottom topography, structural information, average bottom slope in the surf zone, wave parameters, hydrodynamic and morphodynamic time steps, material properties, sediment transport, and morphology options.

The first step of the Q-2DH model involves the computation of nearshore wave heights and mean directions, which are kept constant for a given hydrodynamic time step until bathymetrical changes affect the wave characteristics. The user defines the hydrodynamic time step (Δt). In the second step (STD), the bulk LST rate computed using the extended CERC formula [39] is distributed over the surf zone. Additional transport mechanisms, namely cross-shore, swash zone, and alongshore diffusivity, are utilized herein to maintain the equilibrium beach profile, restrain the growth of small-scale noise, and consider the swash zone profile. In the final step (MEV), the bathymetry is updated using the computed sediment fluxes in a continuity equation. The model structure is shown in Figure 1a. The Q-2DH model uses three different computational grids: i) a primary grid system to compute morphological changes and wave parameters, ii) a staggered grid system interpolated from the primary grid to compute the topographical orientation of the primary grid and the local wave approach angle, and iii) a face-center grid to define sediment influxes and outflux in the x- and y-directions. The grid system is shown in Figure 1b.

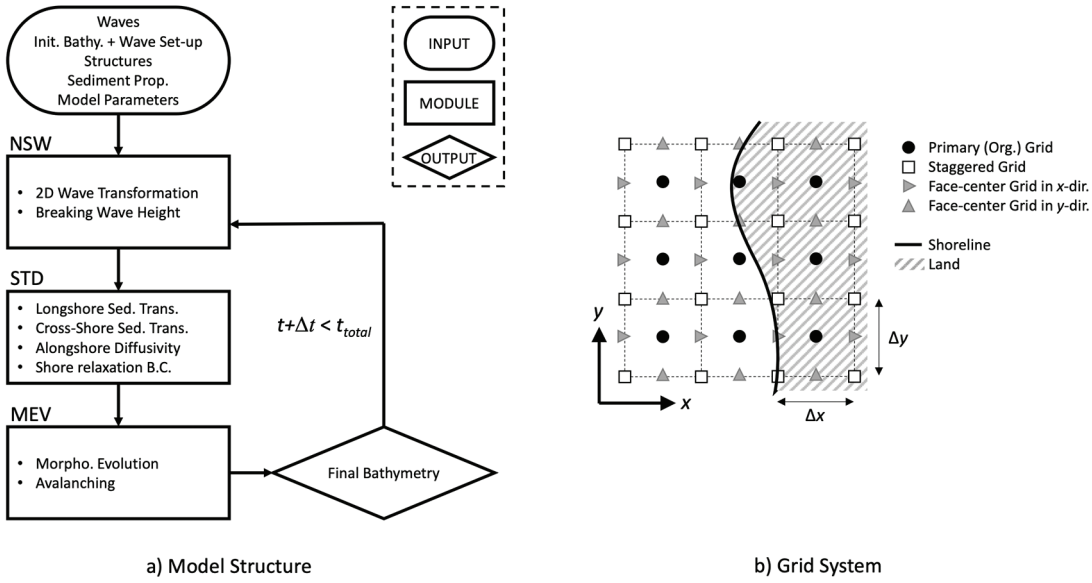

Figure 1. *a) Q-2DH model structure and b) grid system*

NSW: Nearshore spectral wave, STD: Sediment transport distributions, MEV: Morphology evolution, 2D: Two-dimensional

The directional domain is discretized into finite angular grids to describe the spectral density [40].

2.2. Wave Transformation (NSW)

NSW is a phase-averaged 2D spectral wave model [35,38,40], which only solves the energy balance equation in the spatial and directional (-π/2 to π/2) domains. The model considers the following essential processes: linear wave shoaling and refraction, random wave breaking [41], and diffraction [12]. The numerical solution scheme, boundary conditions, and benchmark studies conducted for the module are already given in the literature [35,38,40]. Therefore, they are not provided here for brevity.

2.3. Sediment Transport Distributions

The STD module is where the Q-2DH model's sediment transport computations are carried out. The bulk LST in the module is distributed over the surf zone from the shoreline to the closure depth. The cross-shore sediment transport is computed to preserve the equilibrium beach profile on a relatively long-time scale. Alongshore diffusivity transport is used to restrain the growth of small-scale noise in the MEV module. Furthermore, shore relaxation boundary condition mimics swash zone transport, favoring the profile at the shoreline to evolve to the equilibrium profile.

2.3.1. Longshore sediment transport

The longshore sediment transport (LST) is the primary mechanism in the Q-2DH model. It is calculated following the extended CERC formula [39], which includes the breaking wave height's alongshore gradients [42]:

$$Q = \mu H_{rms,b}^{5/2}\left(\sin(2\beta_b) - \frac{2r}{m}\cos(\beta_b)\frac{\partial H_{rms,b}}{\partial y}\right) \quad (1)$$

Here, Q is the bulk LST, μ is a constant taken as 0.2 $m^{1/2}/s$ (within a range of 0.06-0.45 $m^{1/2}/s$, given by Komar [39]), $H_{rms,b}$ is the root-mean-square breaking wave height, β_b is the angle between the breaking wave approach angle and the bottom contour, the r is a constant equal to 1.0, m is the mean bottom slope at the surf zone, and y is the alongshore distance of the model domain.

The above-given transport formula predicts the bulk LST along the cross-shore profile; thus, it is not directly applicable in a 2D model. The present model is modified to give an order of magnitude for LST at a given point in the computational domain. First, the angle between the breaking wave angle and shoreline (β_b) is replaced with the angle $(\beta = \theta - \alpha)$ between the local wave angle (θ) and the local bottom orientation angle (α) in the model. Figure 2 shows the local bottom orientation (α), local incoming wave angle (θ), and relative incoming angle (α).

Second, the root-mean-square breaking wave height, $H_{rms,b}$, is defined as the most offshore wave height that conforms $H_{rms} \geq \gamma_b \cdot d$ condition, where H_{rms} is the local root mean square wave height. As for the root-mean-square breaking wave height used in the gradient term in Equation (1), the local root-mean-square wave heights are used. The γ_b is the breaking wave index (the ratio of breaking wave height to the breaking water depth) computed using Nairn [43], and d is the local water depth. H_{rms} is the local root-mean-square wave height, calculated using Battjes and Groenendijk [44]

using the significant wave height (H_s) computed by the NSW module at each computational point.

$$\gamma_b = 0.39 + 0.56 \cdot \tanh\left(\frac{33H_{rms,0}}{1.56T_s^2}\right) \quad (2)$$

$$H_{rms} = \left(0.6725 + 0.2025\left(\frac{H_s}{d}\right)\right)H_s \quad (3)$$

Here, $H_{rms,0} = H_{s,0}/\sqrt{2}$ is deep water root-mean-square wave height and T s is significant wave period. Following the above-given computations for bulk LST in the computational domain, the local orientation of the bottom contours, wave height, and approach angle variations due to structures or bathymetric features are considered. van den Berg et al. [25] assumed that the cross-shore distribution of LST roughly follows the longshore current profile and utilized the equation introduced by Komar [39]. However, this approach does not apply to complex coastal defense systems. Therefore, to confine the LST from the shoreline to the closure depth and compute the longshore sediment fluxes at the face centers of the primary grid around the coastal structures, Komar's [39] equation is approximated as follows:

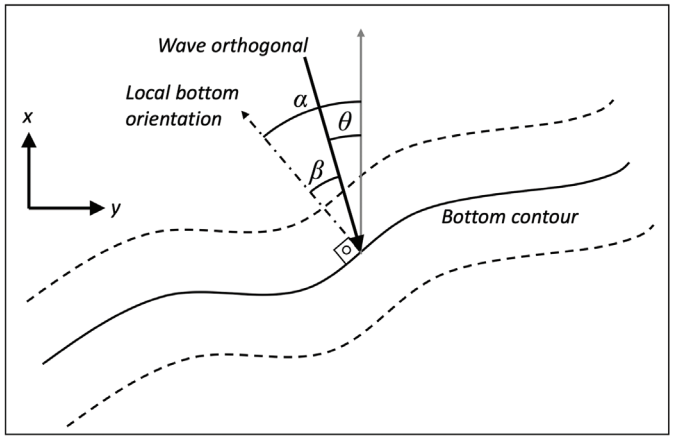

Figure 2. *Angle between local wave angle and local bottom orientation*

$$q_{lst,x} = -Q_{lst} \cdot \overline{C_3} \cdot sin\,(\alpha) \quad (4)$$

$$q_{lst,y} = Q_{lst} \cdot \overline{C_3} \cdot \cos\,(\alpha) \quad (5)$$

$$C_3 = (C_1)^4 \cdot C_2 \quad (6)$$

$$C_1 = \frac{d_c - d}{d_c} \quad (7)$$

$$C_2 = \left(\frac{H_{rms}}{H_{rms,b}}\right)^{5/2} \quad (8)$$

Above, $q_{lst,x}$ and $q_{lst,y}$ are the LST rates computed at each face-center grid location in the x- and y-directions, respectively, depending on the orientation of bottom contours (i.e., for straight parallel bottom contours aligned in the y-direction, $q_{lst,x}$ values become null), d_c is the depth of closure computed with [45] using deep water

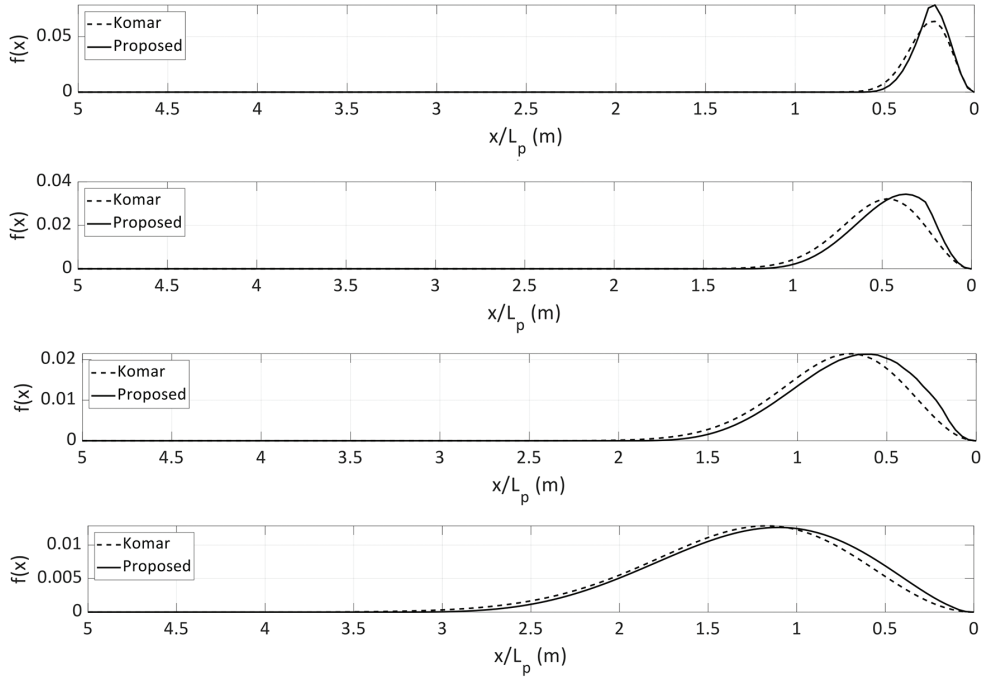

Figure 3. *Comparison of the proposed and Komar [39] (1998) distribution: a) 1/10 slope, b) 1/20 slope, c) 1/30 slope, and d) 1/50 slope*

significant wave height and respective significant period, $\overline{C_3}$ is the normalized distribution over the surf zone. Figure 3 shows the proposed and Komar's distributions [39] for a straight parallel beach with 1/10, 1/20, 1/30, and 1/50 bottom slopes. Here, the $f(x)$ represents the density function of the LST distribution over the surf zone.

In Figure 3, for the bottom slopes of 1/10 and 1/20, the proposed distribution gives slightly higher peak densities than Komar [39] by approximately 20% and 7%, respectively. Both distributions are almost identical qualitatively and quantitatively for the bottom slopes of 1/30 and 1/50. Equations (6-8) agree with Komar [39] with a coefficient of correlation, $R^2 = 0.993$, and a mean absolute error of 5.9% for the above-given bottom slopes. Further study could be conducted to validate these equations using laboratory and field data available in the literature. However, such a study has been kept out of scope in this study.

2.3.2. Cross-shore sediment transport

In the Q-2DH model, cross-shore sediment transport is defined to preserve the equilibrium profile, as given in [25]. The analyses of short- and medium-term events such as storm-induced erosion and breaches or winter and summer profiles are not focused in the Q-2DH model. The parameterization of the cross-shore sediment transport is given as follows:

$$q_{crs} = -\gamma_x \left(\frac{\partial (d - d_e)}{\partial x} \right) \tag{9}$$

$$\gamma_x = \varepsilon_x \gamma_b^{-1/6} g^{1/2} H_{rms,b}^{11/6} X_b^{-1/3} \varphi(x) \tag{10}$$

$$\varphi(x) = \frac{1 + b + \tanh\left(\frac{X_l - x}{L_d}\right)}{1 + b + \tanh\left(X_l / L_d\right)} \tag{11}$$

in which, d is the local depth, d_e is the assumed equilibrium profile depth, γ_x is cross-shore diffusivity constant, ε_x is a non-dimensional constant, γ_b is breaking wave index, g is the gravitational acceleration, $H_{rms,b}$ is the breaking root-mean-square wave height, X_b is the width of the surf zone ($X_b = H_{rms}/(\gamma_b \cdot m)$), $\varphi(x)$ is the shape function. The shape function, $\varphi(x)$, peaks in the surf zone and reduces to a residual value (b) almost equal to zero. The b is a constant controlling the residual magnitude beyond the closure depth, $X_l = 2X_b$, x is the distance to the shoreline in the x-direction, L_d and controls the length scale decay until X_l. The above approach indicates that if the initial profile is identical to the user-defined equilibrium profile, the cross-shore transport is null at the start of the simulation. If the cross-shore profile differs from the equilibrium profile, this profile is altered to the equilibrium profile with non-null cross-shore sediment fluxes.

2.3.3. Alongshore diffusivity

The alongshore diffusivity transport is defined by [25] to mitigate the morphodynamic instabilities in the MEV module. This transport mechanism is based on the local bathymetrical orientation and depth variation in the x- and y-directions. The alongshore diffusivity transport is given below;

$$q_d = -\gamma_y \left(\frac{\partial d}{\partial x} sin(\alpha) + \frac{\partial d}{\partial y} cos(\alpha) \right) \tag{12}$$

where, γ_y is the alongshore diffusivity term, which is similar to the cross-shore diffusivity term, γ_x. The alongshore diffusivity constant is calculated using Equation (10); where ε_x is used instead of ε_y.

2.3.4. Swash zone dynamics

Two distinct methodologies were employed to represent the dynamic behavior of the swash zone in the model. First, a shore relaxation boundary condition is introduced at the shoreline [25], which moves the sediment from wet to dry or in the opposite direction at the shoreline. This boundary condition ensures the preservation of the equilibrium profile at the shoreline so that the bed slope between the wet cell at the shoreline and the adjacent dry cell matches the equilibrium profile. Such a boundary condition is implicitly present in the cross-shore transport definitions of Kristensen et al. [15] and Arriaga et al. [46], which preserve the equilibrium beach profile in their models. Second, a wave-induced setup is calculated using [47] and applied to the entire model domain, leading to the inundation of the swash zone and activating the transport mechanisms in this domain. Such a definition further extends the preservation of the equilibrium onshore, similar to the definition of the berm height limit in Kristensen et al. [15] or the swash zone width in Arriaga et al. [46]. While the first method replicates the behavior of the swash zone, the latter causes the shoreline to move toward the land during wave conditions, thus preserving the equilibrium profile.

Shore relaxation defines sediment transport from wet to dry grid points when the swash zone slope is gentler than the equilibrium slope at the shoreline. As a result, the shoreline advances in the offshore direction. In contrast, if the equilibrium slope is milder than the swash zone slope, sediment transport occurs from dry to wet grid points, resulting in the shoreline retreating landward. The shore relaxation transport is given by;

$$q_{rel} = -\gamma_s \left(\frac{\partial d}{\partial x} cos(\alpha_s) - \frac{\partial d}{\partial y} sin(\alpha_s) + m_s \right) \tag{13}$$

$$q_{rel,x} = -q_{rel} \cdot cos(\alpha_s) \quad (14)$$

$$q_{rel,y} = -q_{rel} \cdot sin(\alpha_s) \quad (15)$$

where, γ_s is the shore relaxation coefficient proportional to $(\Delta x^2)/T_r$, T_r is the relaxation time, d is the local water depth, α_s is the local orientation angle at the shoreline, and m_s is the local bottom slope at the shoreline. Goda [47] provides a relationship to compute the wave-induced setup for a uniform bottom slope range of 1/10-1/100, a wave steepness range of 0.005-0.08, and a wave approach angle range of 0°-70°. The formula is not given here for brevity.

2.4. MEV

In the MEV module, sediment transport rates computed in the STD module at the face centers are used to compute the depth changes:

$$\frac{\partial d}{\partial t} = m_f \left(\frac{\partial q_x}{\partial x} + \frac{\partial q_y}{\partial y} \right) \quad (16)$$

Above, t is time, m_f is the morphological acceleration factor, q_x is the total sediment flux in the x-direction, and q_y is the total sediment flux in the y-direction, where both include the bed porosity factor. The MEV module also has an avalanching algorithm adopted from [38]. The algorithm ensures that the bottom slopes over the computational domain are lower than the critical slopes defined by the user for wet and dry grid points. The default values for the wet and dry critical slopes are 1:6 and 1:5, respectively. Further details are provided in the latter reference.

2.5. Boundary Conditions

The local orientation angles (α) are refined in the model to smoothen the sediment transport direction locally, considering the overall transport direction around a local grid point. This particularly helps to handle cases where the shoreline evolves, having a curvature leading to minimal values of wave approach angles near the shoreline and variations in the sediment transport direction. For the computation of the orientation of the coastline, van den Berg et al. [25] suggested using the mean bathymetric orientation in the surf zone rather than the shoreline orientation or the respective contour orientation. They compute each grid point's mean orientation within a user-defined moving box. Such a moving box filter is applied in the Q-2DH model similarly to [25] to represent the overall sediment transport more accurately. The user defines the moving filter box's dimensions in the order of the surf zone width (X_b), where the default values are two times in the cross-shore direction and four times alongshore.

In the STD module, sediment transport fluxes are computed at the face centers of the primary grid. The most offshore limit of the transport modes is the closure depth. Beyond the closure depth, sediment transport is assumed to be null. On land, the wet cells above a minimum depth (including wave set-up) defined by the user are the most onshore limit of the sediment transport, except for the shore relaxation term. This is intentionally defined in the exact position of the shoreline. The model implements a Courant-Friedrichs-Lewy type [25] numerical stability criterion to control the time increment (Δt) as given below,

$$\Delta t = c H_{rms}{}^{-3/2} \frac{(min\{\Delta x, \Delta y\})^2}{max\{\varepsilon_x, \varepsilon_y\}} \quad (17)$$

where c is a calibration constant with a default value of 0.13, Δx, and Δy are spatial resolutions in the x and y directions, respectively, ε_x and ε_y are non-dimensional constants in Equation (17) with default values of 0.05.

3. Model Application

This section introduces the theoretical case for testing the cross-shore module, the laboratory experiments [37] to which the Q-2DH model is applied, and the methodology for evaluating the differences between the computed and measured results.

Before applying the model to laboratory experiments [37], the model's cross-shore module is first tested with a theoretical case study. A randomly determined initial bed profile is introduced in the model. A LST is absent (perpendicular wave approach), and default values are used for all parameters. The evolution of the initial bottom profile is evaluated. Later, the Q-2DH model was applied to a series of laboratory experiments [37], which were specifically conducted to gather data sets for validating sediment transport relationships and developing computational model algorithms to estimate tombolo processes near headland structures such as offshore breakwaters and T-groins. The experiments consisted of five series of physical model experiments, each including several subseries in which waves and currents were generated on a movable bed in the wave basin. The experiments collected wave heights, current velocities, mean water elevations, bulk sediment transport rates, and bathymetrical data. Among the series, those conducted to obtain data sets for tombolo development at the lee-side of an offshore breakwater are "test 1" and "test 2". In this study, the Q-2DH model is applied to "test 1" only. The "test 1" cases were studied in a subseries of eight simulations (T1C1 through T1C8), with each subseries approximately 190 min long. The cases were conducted on a natural beach with a 4-m-long rubble mound offshore breakwater located 4 m from the initial shoreline and at the center in the alongshore direction (Y=26 m to Y=22 m).

The experiments demonstrated the initiation of a salient in T1C1 and to inspect the advancement of the salient between cases T1C1 and T1C7. In case T1C8, the formation of a tombolo was observed. Furthermore, an additional simulation started from the beginning of case T1C1 and continued almost until the end of case T1C2 without interruption due to any stability problem. Wave-induced longshore currents were recirculated in the basin from downstream to upstream using pumps. Following subseries T1C2 (time=6 hours) and T1C5 (time=15 hours), the sediment traps at the downstream are cleared, and the equilibrium beach profile is reconstructed. The sediment bottom is composed of well-sorted quartz sand with a median grain size of 0.15 mm. The properties of all simulations are given in Table 1. This simulation is named as T1C1-T1C2. The layout of the "Test 1" case is shown in Figure 4.

Table 1. *Benchmark cases*

Case name	$H_{s,0}$ (m)	T_s (s)	θ_0 (°)	Duration (min)	Purpose
Cross-shore transport	0.27	1.43	10	334	Preservation of the equilibrium profile
T1C1	0.27	1.43	10	185	Formation of the salient (model calibration)
T1C2				181	Advancement of the salient
T1C3				185	″
T1C4				192	″
T1C5				176	″
T1C6				189	″
T1C7				191	″
T1C8				184	Formation of the tombolo
T1C1-T1C2				366	Formation of the salient

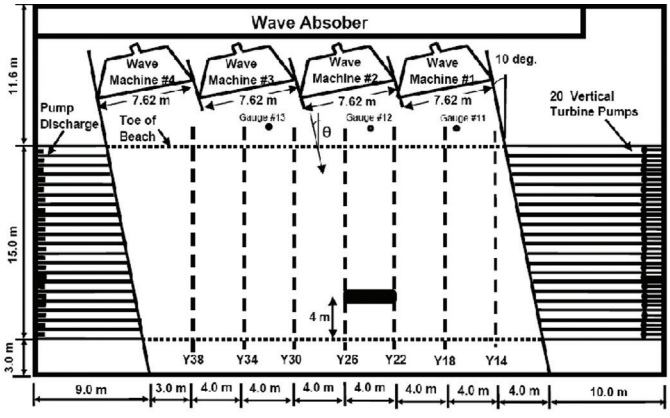

Figure 4. *Initial layout of Test 1 (adopted from Gravens and Wang [37] 2007)*

The computed wave heights were assessed using an aerial mean absolute percent error (MAPE) definition. The results of beach evolution were evaluated using both MAPE and Brier Skill Score (BSS) [48]. For morphological evaluations, the MAPE is computed separately for the shoreline change and bathymetry. MAPE is given in Equation 18:

$$MAPE = \frac{1}{n}\sum_{i=1}^{n}\left|\frac{y_i - x_i}{x_i}\right| \tag{18}$$

where y_i is the predicted value, x_i is the true value, and n is the total number of data points.

BSS is a score function commonly used in sediment transport and beach evolution modeling. It computes the mean squared difference between the observed and predicted values. A BSS score equal to one gives an excellent correlation, which worsens as the value decreases below zero. The BSS is given by Equation 19:

$$BSS = 1 - \frac{\sum_{i=1}^{n}\sum_{j=1}^{k}\left(d_{i,j}^{p} - d_{i,j}^{m}\right)^2}{\sum_{i=1}^{n}\sum_{j=1}^{k}\left(d_{i,j}^{b} - d_{i,j}^{m}\right)^2} \tag{19}$$

with $d_{i,j}^{p}$ is the predicted depth at the (i, j)th cell, $d_{i,j}^{m}$ is the measured depth at the (i, j)th cell and $d_{i,j}^{b}$ is the initial depth at the (i, j)th cell. According to van Rijn et al. [49] (2003), the performance of a morphologic simulation is considered as "bad" when $BSS<0.0$, "poor" when $0.0<BSS<0.1$, "reasonable/fair" when $0.1<SS<0.2$, "good" when $0.2<BSS<0.5$, and excellent" when $0.5<BSS<1.0$. In the BSS computation, only the offshore breakwater's lee side is considered. van Rijn et al. [49] state, "BSS is susceptible to small changes when the denominator is low". When considering the entire model domain, depths with minimum differences in the model and measurements lead to lower BSS scores. Therefore, BSS is calculated for three different depth intervals (0-0.08 m, 0.08-0.16 m, and 0-0.16 m), which will be addressed further as BSS1, BSS2, and BSS3, respectively, in each case. BSS3 gives a score for the entire region at the lee side of the breakwater.

The T1C1 case lasted 185 min with waves and wave-induced currents. The Q-2DH model is first calibrated for the T1C1 case, and the calibrated parameter values are used in subsequent cases. The model domain area is discretized with an equal grid spacing of 0.2 m in both the alongshore and cross-shore directions following Nam et al. [50] and Baykal et al. [35]. To sustain the longshore currents in the model area, the model area is extended 20 m in the upstream and downstream directions. These extended lateral boundaries are not considered in the MAPE and BSS computations. The

model domain is also extended in the offshore direction by extrapolating the water depths from the most offshore depth of T1C1 as 0.7 to an offshore depth of 1.69 m to satisfy the offshore wave conditions of Test 1. In summary, the model area is composed of a total of 113 cells (X-range=1.6 to 24) in the x-direction and 301 cells (Y-range=-6 to 54) in the y-direction. Other model parameters are listed as follows: $H_{s,0}$=0.27 m, $T_{s,0}$=1.42, θ_0=10°, γ_b=0.78, s_{max}=10, ε_x=0.5, ε_y=0.5, γ_s=6.24*10-6, m_f=0.37, μ=0.20, d_c=0.37 m and Δ_t=0.2 s. The $H_{s,0}$, $T_{s,0}$, θ_0, γ_b and s_{max} are adjusted to assure the offshore wave conditions of T1C1. The parameters ε_x, ε_y, γ_s and m_f are calibrated by trial and error until the computed shoreline agrees quantitatively and qualitatively with the measured shoreline in T1C1. As mentioned earlier, the Δ_t is the hydrodynamic time step satisfying the stability criterion. For the computation of the mean orientation of the coastline, the dimensions of the moving box filter are introduced as two times the surf-zone width in the alongshore direction and one surf-zone width in the cross-shore direction.

4. Results and Discussion

The results of the simulations introduced in the preceding section are given and discussed in this section.

4.1. Cross-Shore Transport

In the Q-2DH model, a parametrized expression for cross-shore sediment transport is applied rather than a process-based method. This parameterized expression restores or preserves the predefined equilibrium profile on a relatively long-time scale. Here, the simulation results are given, where the sediment transport is in the cross-shore direction only and the alongshore transport is not present. The bottom profiles of different time steps are shown in Figure 5, where the black solid line represents the initial profile, the black dashed line represents the bottom profile at the respective time step, and the red dashed line represents the user-defined equilibrium profile.

In Figure 5a (t=0 seconds), the initial and final profiles are identical, as cross-shore sediment transport has not yet started. In Figure 5b (t=1000 seconds), the profile approximately takes the shape of the equilibrium profile. In Figure 5c (t=10000 seconds), the final profile is almost identical to the equilibrium profile. In Figure 5d (t=20000 seconds), the final and equilibrium profiles are similar. It can be inferred that the magnitudes of the fluxes are much higher in the earlier steps of the simulation and gently decrease to null.

4.2. Laboratory Experiments

In the simulations of the laboratory experiments, the model is first applied to the case T1C1. The variation of significant wave heights in the cross-shore direction for the Y30 and Y24 profiles, the alongshore direction for the X5.2 profile, and the a LST flux variation for the Y24 profile are shown in Figure 6.

Figure 6 shows that the computed significant wave heights agree with the measurements. The wave heights in the shadow zone right behind the breakwater are underestimated

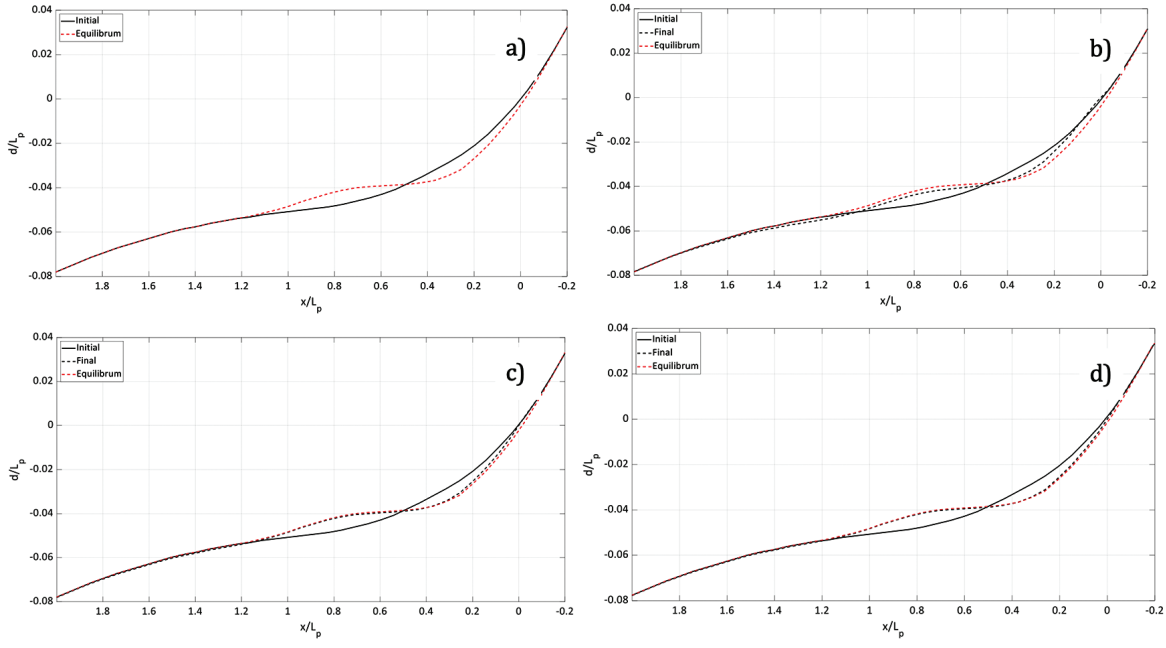

Figure 5. *Evolution of bottom profile under cross-shore sediment transport a) t=0 s, b) t=1000 s, c) t=10000 s, and d) t=20000 s. The solid line is the initial bottom profile, the red dashed line is the equilibrium bottom profile, and the black dashed line is the intermediate bottom profile*

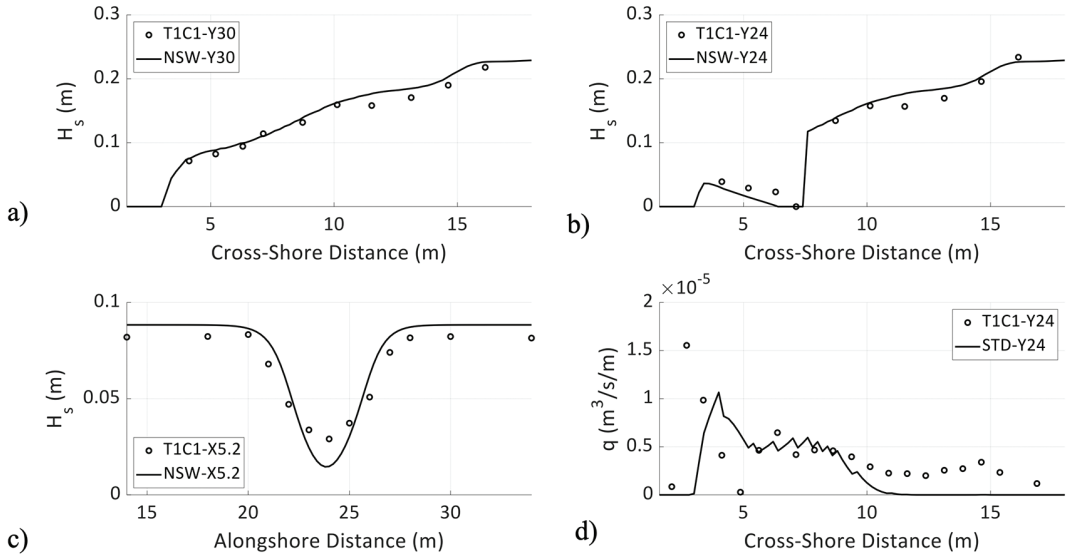

Figure 6. *a) Significant wave heights along Y30, b) Y24, c) X5.2, and d) longshore sediment fluxes at Y24. The circles represent the measurements. The solid line is computed*

NSW: Nearshore spectral wave, STD: Sediment transport module

by almost 20% on average (22 m<Y<26 m). Meanwhile, they are slightly overestimated by 5% on average in the illuminated zone (Y<22 m and Y>26 m). The MAPE for the significant wave heights for T1C1 is computed as 12%. The alongshore bulk sediment fluxes are in relatively good agreement with the measurements around the offshore breakwater; however, they are underestimated close to the shoreline and further offshore. For the other tests (T1C2-T1C8), the computed significant wave heights are compared with the measurements in Figures 7 and 8. The MAPE values were calculated for the significant wave heights, shoreline, and bathymetry, the BSS scores computed for various depth ranges, and the relative maximum shoreline retreat and advancement (R_{rel} and A_{rel}, respectively) in shore-normal directions computed and measured for all simulations are shown in Table 2. The values of the shoreline retreat and advancement given in Table 2 are determined for each simulation from the initial and final positions of the shoreline in each case.

In Figures 7 and 8, solid black lines are the equal height contours of significant wave heights measured by [37], gray dotted lines are computed by the Q-2DH model, and blue dotted lines are the initial bottom contours of the respective tests. As seen from the figures, the computed significant wave heights agree well with the observations around the structure both quantitatively and qualitatively. For all cases, the wave heights in the shadow zone of the breakwater (4<X<6 m and 22<Y<26 m) are slightly underestimated, whereas in the illuminated zone, they are overestimated. Overall, the MAPE values varied between 11% and 18% (see Table 2), where the maximum differences are observed for T1C7 and T1C8 (final stages of salient before tombolo formation), and the minimum discrepancies are observed for T1C3 and T1C2 (early stages of salient).

The morphological changes computed by the Q-2DH model are compared with the measurements in Figures 9 and 10 for the cases T1C1-T1C8. In the figures, the solid black lines are the bottom contours measured by [37], the gray dotted lines are the computed bottom contours by the Q-2DH model, and the blue dotted lines are the initial bottom contours of the respective tests. In Figure 9a, for the T1C1 case, the shoreline and 0.1 m contour computed by the model match well with the measured contours. There are some irregularities in the bottom contours at the sides of the salient and offshore breakwater. Moreover, the 0.1 m contour is aligned toward the left in the measurements, whereas the computed contour is more symmetrical. Figure 9b shows that the Q-2DH model overpredict the accretion at the shoreline in the T1C2 case, whereas the computed 0.1 m contour is close to the measurement. In the T1C3 case (Figure 9c), the computed shoreline is identical to the experimental results. Both the computed and measured 0.1-m contours merge with the 0.1-m contour around the breakwater on the left side of the breakwater. In the T1C4 case (Figure 9d), the contour lines are quantitatively and qualitatively similar at the lee side of the breakwater. More scour occurs on the left and right sides of the breakwater than in the observations. In T1C5 (Figure 10a), the shoreline recedes more in the model results than in the experiments. Figure 10b shows that the shoreline and 0.1 m contour are similar to the observations of T1C6. At the updrift (left) part, the shoreline and 0.1 m contour are much more accreted than in the model, whereas erosion are

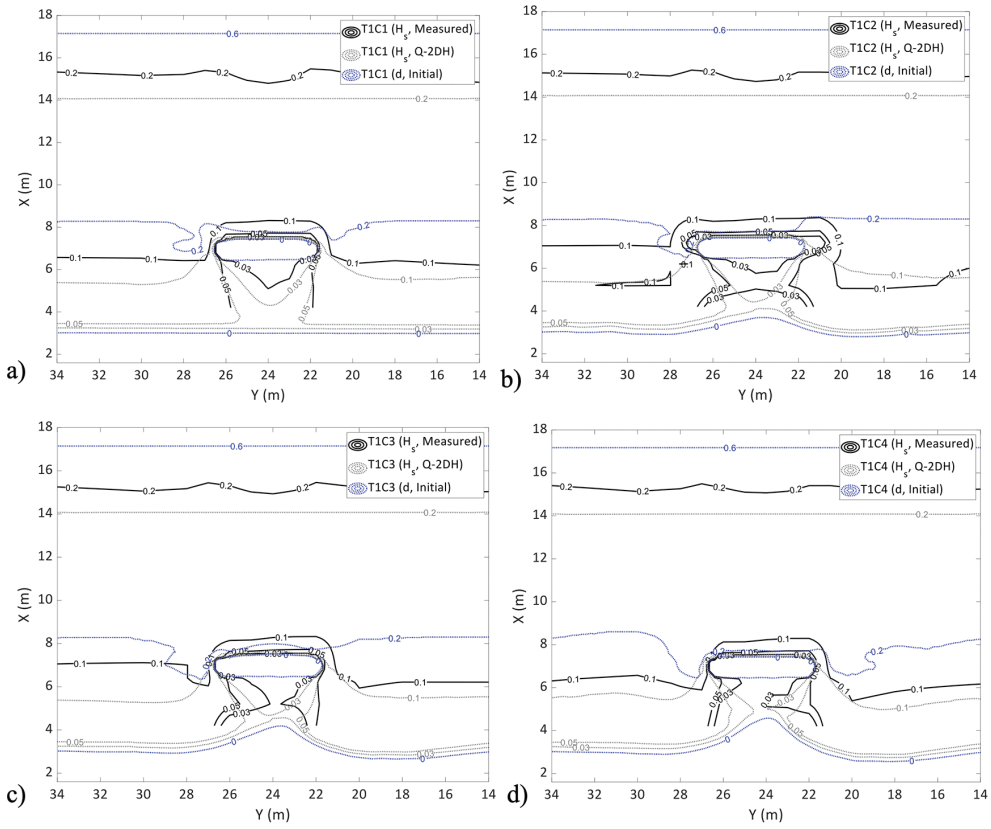

Figure 7. *Measured and computed significant wave heights for the tests: a) T1C1, b) T1C2, c) T1C3, and d) T1C4. (Solid black lines are measured by Gravens and Wang [37], gray dotted lines are computed by the Q-2DH model, and blue dotted lines are the initial bottom contours)*

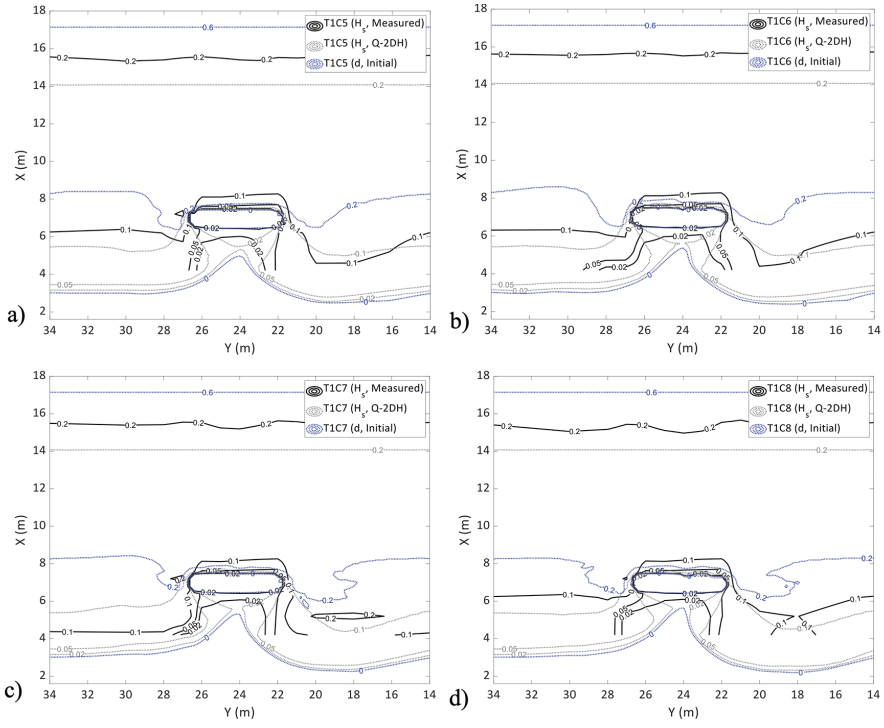

Figure 8. *Measured and computed significant wave heights for the tests: a) T1C5, b) T1C6, c) T1C7, and d) T1C8. (Solid black lines are measured by Gravens and Wang [37] 2007; gray dotted lines are computed by the Q-2DH model, and blue dotted lines are the initial bottom contours)*

Table 2. *MAPE for significant wave heights, bathymetry and shoreline, BSS scores, and shoreline retreat and advancement near the breakwater*

Case name	MAPE			BSS1*	BSS2**	BSS3***	Measured		Computed	
	H_s	Bathymetry	Shoreline				R_{rel} (m)	A_{rel} (m)	R_{rel} (m)	A_{rel} (m)
T1C1	0.12	0.26	0.0024	0.83	0.62	0.71	0.29	0.88	0.39	0.83
T1C2	0.12	0.37	0.0011	0.71	-0.45	0.50	0.34	0.48	0.25	1.00
T1C3	0.11	0.29	0.0026	-1.26	0.07	-0.42	0.11	0.43	0.24	0.85
T1C4	0.14	0.22	0.0068	-1.45	-0.03	-0.65	0.14	0.43	0.33	0.72
T1C5	0.16	0.29	0.0019	-2.93	-0.91	-2.00	0.25	0.38	0.30	0.41
T1C6	0.15	0.22	0.0067	-2.78	-1.21	-2.22	0.47	0.13	0.37	0.15
T1C7	0.18	0.28	0.0036	-8.47	-2.99	-6.43	-	-	-	-
T1C8	0.16	0.31	0.0100	-7.93	-2.95	-6.07	-	-	-	-
T1C1-T1C2	0.12	0.37	0.0015	0.85	0.58	0.74	0.38	1.27	0.52	1.21

*: Calculated for 0-0.08 m depth range, **: Calculated for 0.08-0.16 m depth range, ***: Calculated for 0-0.16 m depth range MAPE: Mean absolute percent error, BSS: Brier Skill Score

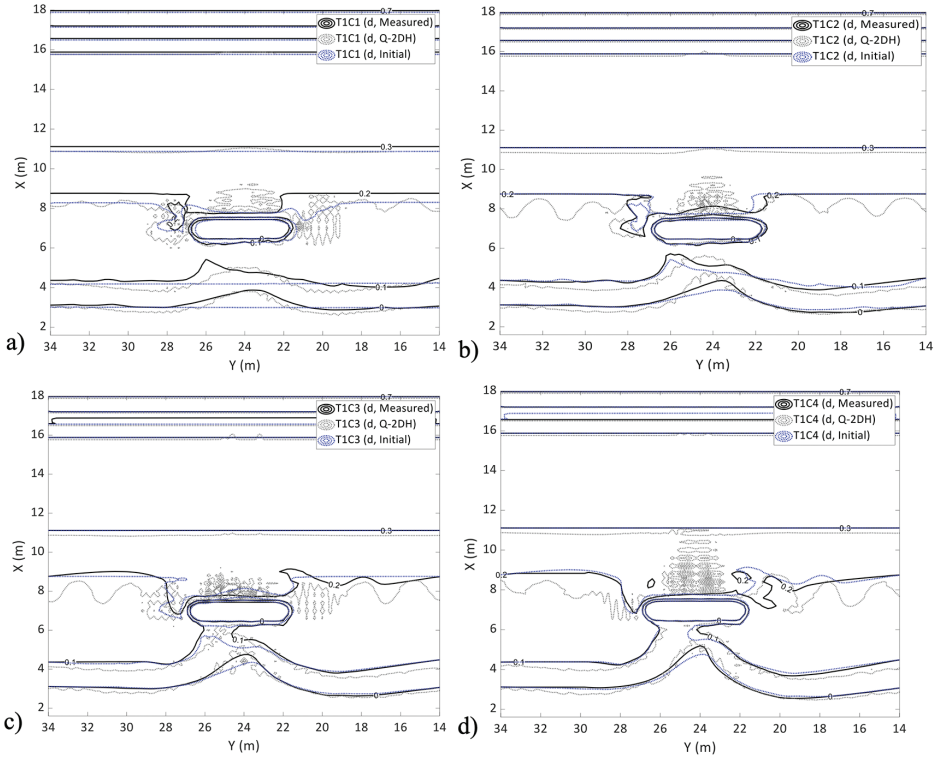

Figure 9. *Measured and computed bottom contours for the tests: a) T1C1, b) T1C2, c) T1C3, and d) T1C4. (Solid black lines are measured by Gravens and Wang [37], gray dotted lines are computed by the Q-2DH model, and blue dotted lines are the initial bottom contours)*

similar at the downdrift part (right side). In the T1C7 case (Figure 10c), the model results show that the shoreline does not progress toward the breakwater; its alongshore width increases. The computed 0.1 m contour is similar to the experimental result. Finally, for the T1C8 case (Figure 10d), the computed shoreline is a partial tombolo formation with some discontinuities. On the other hand, the computed 0.1 m contour is close to the observation.

As a general tendency, the MAPE values computed for the shoreline for all cases increase with the case number, similar to the wave heights. However, the MAPE values computed for the nearshore bathymetry do not have such a trend and vary between 22% and 37%, with an average value of 28%. BSS scores are more sensitive than MAPE values for areal changes. They follow a similar trend to the MAPE values computed for wave heights. As the number of cases increases,

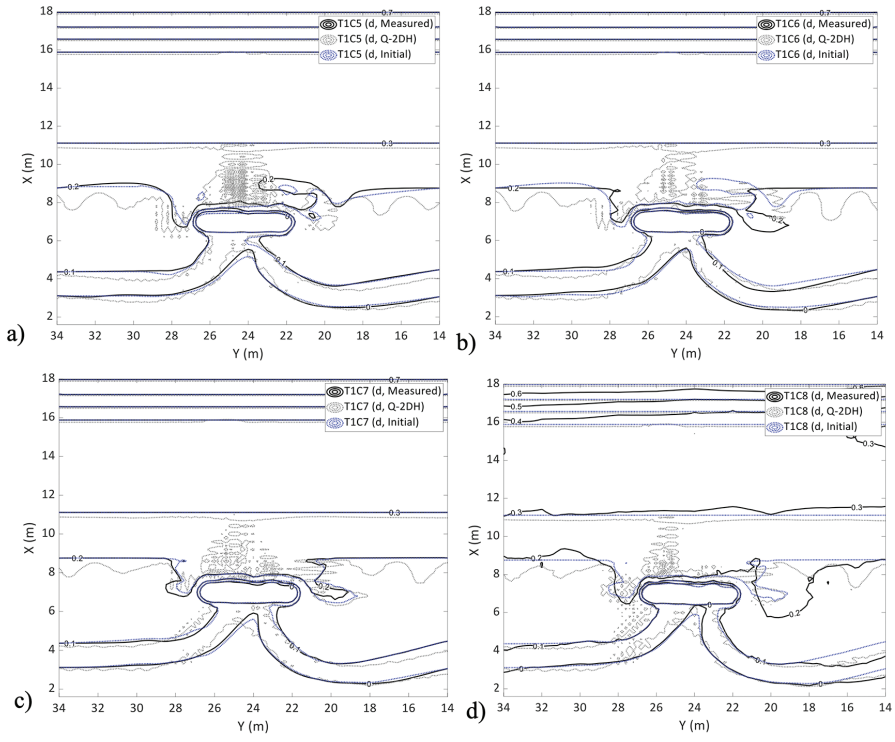

Figure 10. *Measured and computed bottom contours for the tests: a) T1C1, b) T1C2, c) T1C3, and d) T1C4. (Solid black lines are measured by Gravens and Wang [37], gray dotted lines are computed by the Q-2DH model, and blue dotted lines are the initial bottom contours)*

the model's prediction performance decreases, and the BSS values are reduced. This is related to the high orientation angles of the bottom contours occurring as the shoreline advances in the offshore direction toward the breakwater. The highest BSS values were observed in T1C1, T1C2, and T1C1-T1C2, which could be classified as "excellent". The smallest values were obtained for the T1C7 and T1C8 cases. In addition, BSS1 (computed within 0-0.08 m depths) and BSS2 computed within 0.08-0.16 m depths) values computed for all the cases imply that the model performance on computing the morphological changes close to the shoreline (within 0-0.08 m depths) is slightly better than the rest of the nearshore domain. Table 2 shows that the model predicts the maximum relative shoreline retreat and advancement in the shore-normal direction with relatively good accuracy for the T1C1 case and the continuous run T1C1-T1C2. However, as the shoreline advances in the normal direction, the computed values become larger than the measured. This might be attributed to the wave heights being underestimated in the shadow zone, thus resulting in larger alongshore transport gradients moving the sediment toward the lee side of the breakwater. After the 0.1-m contour merges toward the detached breakwater, the retreat and advancement values become close again.

The Q-2DH model is also run from the start of the experiments (T1C1) with the same settings and parameter values until it is interrupted due to an instability error, which is almost equivalent to the end of T1C2. The run is named T1C1-T1C2. The total model run time is 366 min. The computed bathymetry was compared with the experimental results (T1C2 final bathymetry). The computed significant wave heights for this run are almost the same as those for the T1C1 case, as shown in Figure 7a. A comparison of the

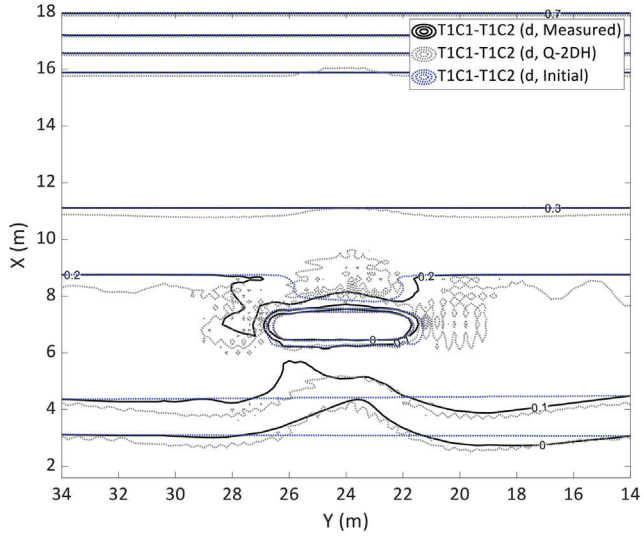

Figure 11*. Comparison of bottom contours for T1C1-T1C2 (measured) and T1C1-T1C2 (Q-2DH).*

measured and computed bottom contours for the T1C1-T1C2 simulation is given in Figure 11.

Figure 11 shows that the shoreline and 0.1 m contour are similar to the observations. At the updrift (left) part, the two measured contours accreted more than the model. At the downdrift part (right side), erosion are similar; however, around Y18, the measured contours are positioned offshore compared to the computed ones.

5. Conclusion

In the present study, a quasi-2-dimensional numerical model developed to simulate both medium- and long-term shoreline changes under wave action near coastal structures is applied to the experimental dataset of [37] on shoreline evolution behind an offshore breakwater. The model provides a more precise wave transformation computation than the one-line models. At the same time, it demands a smaller number of input parameters and fewer computational sources compared with complex 2DH and 3D models, eliminating complex nearshore circulation and advection-diffusion computations.

The model computes the wave field in the vicinity of structures using a spectral wave model [38] rather than geometric/parametric computations as in one-line models. Thus, the accuracy of the wave field is comparable to that of complex models. Then, it computes the distributed LST based on nearshore wave characteristics. The model also incorporates a cross-shore sediment transport algorithm, alongshore diffusivity, and shore relaxation terms [25]. The cross-shore sediment transport algorithm preserves the equilibrium profile. The alongshore diffusivity term eliminates the growth of high-approach angle stability errors. The shore relaxation term mimics swash zone transport. In addition, a wave setup term is adopted from [47] to represent the mean water level variations at the wet/dry interface of the bathymetry and to extend the active zone of sediment transport further onshore (similar to the definition of equilibrium beach profile), which is handled by solving non-linear shallow water equations in complex models and promoting sediment transport around the shoreline.

The model is first applied to a theoretical case in which cross-shore transport is the only governing mode of transport. The cross-shore transport module can restore any user-defined equilibrium beach profile, which is a major assumption of the one-line-based models. Later, the model was applied to laboratory tests [37]. The present study studies the experiments from T1C1 to T1C8 using the Q-2DH model. When the cases are individually studied, the Q-2DH model quantitively and successfully estimates the nearshore wave field and bathymetrical changes for all cases. The MAPE values computed for the shoreline BSS scores give that the model thrives, especially in T1C1, T1C2, and the continuous run T1C1-T1C2 cases. However, in further cases (T1C3 to T1C8), the performance of the Q-2DH model is reduced. As the shoreline progresses toward the offshore breakwater, high local orientation angles and high incoming wave angles occur, resulting in irregularities in morphological computations. As these irregularities accumulate over time, they result in a highly varying bathymetry, which leads the model to fail.

Further studies are required to resolve the high-wave approach and high local orientation angle-led problems. Such studies will enable us to simulate shoreline changes more accurately around shore-normal structures like shore-normal or angled groins and T-groins. Moreover, the curved shorelines/pocket beaches with/without the presence of structures, sand sources/sinks, tides, and currents also stand as further challenges for simpler models like the Q-2DH model.

Authorship Contributions

Concept design: C. Baykal, and C. Özsoy, Data Collection or Processing: C. Baykal, and C. Özsoy, Analysis or Interpretation: C. Baykal, and C. Özsoy, Literature Review: C. Baykal, and C. Özsoy, Writing, Reviewing and Editing: C. Baykal, and C. Özsoy.

Funding: The authors declare that no funds, grants, or other support was received during the preparation of this manuscript.

References

[1] R. Pelnard-Considere, "*Essai de Theorie de L'Evolution des Form de Rivage en Plage de Sable et de Galets*". 4th Journess de l'Hydraulique, Les Energies de la Mer, Question III, Rapoort No. 1, 1956, pp. 289-298.

[2] W. A. Price, D. W. Tomlinson, and D. H. Willis, "*Predicting changes in the plan shape of beaches*". Proceedings of the 13th International Conference on Coastal Engineering, 1973, ASCE.

[3] H. Hanson, and N. C. Kraus, "*Genesis: generalized model for simulating shoreline change*". Technical Report CERC-89-19, Report 2 of a Series, Workbook and User's Manual. US Army Corps of Engineers, Waterways Experiment Station, Vicksburg, MS, 1989, USA.

[4] M. A. Dabees, and J. W. Kamphuis, "*Oneline, a numerical model for shoreline change*". Proceedings 27th International Conference on Coastal Engineering, ASCE, Copenhagen, 1998. pp. 2668-2681.

[5] I. Şafak, "*Numerical modeling of wind wave induced longshore sediment transport*". M.Sc. Thesis, METU, Ankara, Turkey, 2006.

[6] S. S. Artagan, "*A one line numerical model for shoreline evolution under the interaction of wind waves and offshore breakwaters*". M.Sc. Thesis, METU, Ankara.

[7] C. Baykal, "*Numerical modeling of wave diffraction in one-dimensional shoreline change model*". M.Sc. Thesis, METU, Ankara, Turkey, 2006.

[8] M. Esen, "*An implicit one-line numerical model on longshore sediment transport*". M.Sc. Thesis, METU, Ankara, Turkey, 2006.

[9] A. M. Elghandour, "*Efficient Modelling of coastal evolution. Development, verification and validation of ShorelineS model*". Delft: IHE Delft Insitute for Water Education, 2018.

[10] A. Robinet, B. Castelle, D. Idier, M. D. Harley, and K. D. Splinter, "Controls of local geology and cross-shore/longshore processes on embayed beach shoreline variability". *Marine Geology* vol. 422, 106118, Apr 2020.

[11] L. X. Hoan, "*Long-term simulation of coastal evolution*". Ph.D. Thesis, Lund, Sweden, 2010.

[12] H. Mase, "Multidirectional random wave transformation model based on energy balance equation," *Coastal Engineering Journal,* vol. 43, pp. 317-337, May 2001.

[13] G. A. Smith, "*Wave induced sediment mobility modelling: bedforms, sediment suspension and sediment transport*". Ph.D. Thesis, Swinburne University, 2012.

[14] N. Booij, R. sC. Ris, and L. H. Holthuijsen, "A third-generation wave model for coastal regions: 1. model description and validation". *Journal of Geophysical Research: Oceans,* vol. 104, pp. 7649-7666, Apr 1999.

[15] S. E. Kristensen, N. Drønen, R. Deigaard, and J. Fredsoe, "Hybrid morphological modelling of shoreline response to a detached breakwater". *Coastal Engineering,* vol. 71, pp. 13-27, Jan 2013.

[16] DHI, Danish Hydraulic Institute. "*MIKE 21/3 Coupled Model FM. Technical Documentation*". Shoreline Morphology Module, Lyngby, Denmark, 2005.

[17] V. T. Dang, "Development of a mathematical n-line model for simulation of beach *changes*". Ph.D Thesis. University of New South Wales, 2006.

[18] B. A. Ebersole, M. A. Cialone, and M. D. Prater, "*Regional coastal processes numerical modeling system: Report 1: RCPWAVE - a linear wave propagation model for engineering use*", Technical Report CERC 86-4. US Army Corps of Engineers, CERC. Vicksburg, Miss., 1986.

[19] H. Hanson, M. Larson, N. C. Kraus, and M. Capobianco, "*Modeling of seasonal variations by cross-shore transport using one-line compatible methods*", Proceedings, Coastal Dynamics '97, ASCE, pp. 893-902, 1997.

[20] H. Hanson, and M. Larson, "*Seasonal shoreline variations by cross-shore transport in a one-line model under random waves*". Proceedings of 26th International Coastal Engineering Conference, ASCE, pp. 2682-2695, 1998.

[21] M. Larson, N. C. Kraus, and H. Hanson, "*Decoupled numerical model of three-dimensional beach range*". Proceedings 22nd Coastal Engineering Conference, ASCE, pp. 2173-2185, 1990.

[22] H. Hanson, and M. Larson, "*Simulating coastal evolution using a new type of N-line model*". Proceedings 27th Coastal Engineering Conference ASCE, pp. 2808-2821, 2000.

[23] M. A. Dabees, and J. W. Kamphuis, "*NLINE: efficient modeling of 3-D beach change*". Proceedings 27th Coastal Engineering Conference ASCE, pp. 2700-2713, 2000.

[24] T. Shimizu, T. Kumagai, and A. Watanabe, "*Improved 3-D beach evolution model coupled with the shoreline model (3D-shore)*". Proceedings 25th Coastal Engineering Conference ASCE, pp. 2843-2856, 1996.

[25] N. van den Berg, A. Falqués, and F. Ribas, "Long-term evolution of nourished beaches under high angle wave conditions". *Journal of Marine Systems,* vol. 88, pp. 102-112, Oct 2011.

[26] A. Robinet, D. Idier, B. Castelle, and V. Marieu, "A reduced-complexity shoreline change model combining longshore and cross-shore processes: the LX-Shore model". *Environmental Modelling & Software,* vol. 109, pp. 1-16, Nov 2018.

[27] H. Hanson, M. Larson, and N. C. Kraus, "A new approach to represent tidal currents and bathymétrie features in the one-line model concept," Proceedings Coastal Dynamics '01, ASCE, pp.172-181, 2001.

[28] M. Larson, N. C. Kraus, and H. Hanson, "*Simulation of regional longshore sediment transport and coastal evolution - the 'Cascade' model*". Proceedings of 28th Coastal Engineering Conference, World Scientific Press, Singapore, pp. 2612-2624, 2002.

[29] M. Larson, N. C. Kraus, and K. J. Connell, "*Cascade version 1: Theory and model formulation*," ERDC TNSWWRP-06-7. Vicksburg, Mississippi: U.S. Army Engineer Research and Development Center, 2006.

[30] K. Kaergaard, and J. Fredsoe, "*A numerical shoreline model for shorelines with large curvature*". Coastal Engineering, vol. 74, pp. 19-32, Apr 2013.

[31] A. Militello, C. W. Reed, A. K. Zundel, and N. C. Kraus, "*Two-dimensional depth-averaged circulation model M2D: Version 2.0, Report 1: Documentation and user's guide*," ERDC/CHL TR-04-02, U.S. Army Engineer Research and Development Center, Vicksburg, MS, 2004.

[32] A. M. Buttolph, et al. "*Two-dimensional depth-averaged circulation model CMS-M2D: Version 3.0, report 2*". Sediment Transport and Morphology Change. Technical Report ERDC/CHL TR-06-9, Coastal and Hydraulics Laboratory, US Army Engineer Research and Development Center, Vicksburg, MS, 2006.

[33] N. Bruneau, P. Bonneton, R. Pedreros, F. Dumas, and D. Idier, "A new morphodynamic modelling platform: application to characteristic sandy systems of the aquitanian coast, France". *Journal of Coastal Research,* vol. 50, pp. 932-936, 2007.

[34] D. Roelvink, A. Reniers, A. van Dongeren, J. van Thiel de Vries, R. McCall, and J. Lescinski, "Modelling storm impacts on beaches, dunes and barrier islands". *Coastal Engineering,* vol. 56, pp. 1133-1152, Nov-Dec 2009.

[35] C. Baykal, A. Ergin, and I. Güler, "Two-dimensional depth-averaged beach evolution modeling: case study of the Kizilirmak River Mouth, Turkey". *Journal of Waterway Port Coastal and Ocean Engineering,* vol. 140, 2014.

[36] D. Roelvink, B. Huisman, A. Elghandour, M. Ghonim, and J. Reyns, "Efficient modeling of complex sandy coastal evolution at monthly to century time scales". *Frontiers in Marine Science,* 7, 2020.

[37] M. B. Gravens and P. Wang, "*Data report: Laboratory testing of longshore sand transport by waves and currents; morphology change behind headland structures*," Technical Report, ERDC/CHL TR-07-8, Coastal and Hydraulics Laboratory, US Army Engineer Research and Development Center, Vicksburg, MS, 2007.

[38] C. Baykal, "*Two-Dimensional Depth-Averaged Beach Evolution Modelling*," Ph.D. Thesis, METU, Ankara, Turkey, 2012.

[39] P. D. Komar, "Beach Processes and Sedimentation," 2nd Edition. Prentice Hall, Englewood Cliffs, N.J., 1998.

[40] C. Baykal, "Development of a numerical 2-dimensional beach evolution model". *Turkish Journal of Earth Sciences,* vol. 23, pp. 215-231, 2014.

[41] T. T. Janssen, and J. A. Battjes, "A note on wave energy dissipation over steep beaches". *Coastal Engineering,* vol. 54, pp. 711-716, Sep 2007.

[42] H. Ozasa, and A. H. Brampton, "Mathematical modelling of beaches backed by seawalls". *Coastal Engineering,* vol. 4, pp. 47-63, 1980-1981.

[43] R. B. Nairn, "*Prediction of cross-shore sediment transport and beach profile evolution*". Ph.D Thesis, Imperial College, London, 1990.

[44] J. A. Battjes, and H. W. Groenendijk, "Wave height distributions on shallow foreshores". *Coastal Engineering,* vol. 40, pp. 161-182, Jun 2000.

[45] R. J. Hallermeier, "*Uses for a calculated limit depth to beach erosion*". Proceedings 16th International Conference on Coastal Engineering ASCE, New York, pp. 1493-1512, 1978.

[46] J. Arriaga, J. Rutten, F. Ribas, A. Falqués, and G. Ruessink, "Modeling the long-term diffusion and feeding capability of a mega-nourishment". *Coastal Engineering,* vol. 121, pp. 1-13, Mar 2017.

[47] Y. Goda, "Wave setup and longshore currents induced by directional spectral waves: prediction formulas based on numerical computation results". *Coastal Engineering Journal*, vol. 50, pp. 397-440, 2008.

[48] G. W. Brier, "Verification of forecasts expressed in terms of probability". *Monthly Weather Review*, vol. 78, pp. 1-3, Jan 1950.

[49] L. C. van Rijn, D. J. R. Walstra, B. Grasmeijer, J. Sutherland, S. Pan, and J. P. Sierra, "The predictability of cross-shore bed evolution of sandy beaches at the time scale of storms and seasons using process-based profile models". *Coastal Engineering,* vol. 47, pp. 295-327, Jan 2003.

[50] P. T. Nam, M. Larson, H. Hanson, and L. X. Hoan, "A numerical model of nearshore waves, currents, and sediment transport". *Coastal Engineering,* vol. 56, pp. 1084-1096, Nov-Dec 2009.